JET TRANSPORT PROPAGATION OF UNCERTAINTIES FOR ORBITS AROUND THE EARTH

Daniel Pérez[*], Josep J. Masdemont[‡], Gerard Gómez[§]

Abstract

In this paper we present a tool to study the non-linear propagation of uncertainties for orbits around the Earth. The tool we introduce is known as Jet Transport and allows to propagate full neighborhoods of initial states instead of a single initial state by means of usual numerical integrators. The description of the transported neighborhood is obtained in a semi-analytical way by means of polynomials in 6 variables. These variables correspond to displacements in the phase space from the reference point selected in an orbit as initial condition. The basis of the procedure is a standard numerical integrator of ordinary differential equations (such as a Runge-Kutta or a Taylor method) where the usual arithmetic is replaced by a polynomial arithmetic. In this way, the solution of the variational equations is also obtained up to high order. This methodology is applied to the propagation of satellite trajectories and to the computation of images of uncertainty ellipsoids including high order nonlinear descriptions. The procedure can be specially adapted to the determination of collision probabilities with catalogued space debris or for the end of life analysis of spacecraft in Medium Earth Orbits.

1 Introduction

Any trajectory, from the ones of small debris to big asteroids, or artificial satellites, is under uncertainty when its orbit is tried to be determined. As it is well known, small differences in the initial conditions can produce big deviations from predicted states after some time. Therefore it is very important to study how these uncertainties evolve and how can they be controlled along the time.

The study of uncertainties is usually performed by means of Monte Carlo methods or analyzing the evolution of the covariance matrix. The first option, based on massive integrations of initial conditions, has a slow rate of convergence towards a meaningful result. On the other hand, the study of the covariance matrix is a faster method but only takes into account a linear approximation of the uncertainties, while higher order approximations could play an important role.

In this paper we present a new way to study uncertainty regions: The Jet Transport. Given an initial state x_0, the Jet transport consist in the integration of a full neighborhood of states around x_0, instead of doing the single propagation of x_0. This procedure is also known as Differential Algebra and it was introduced by M. Wertz and K. Makino for the study of particle beams and particle accelerators. This kind of techniques have been also applied in celestial mechanics to work with Kalman Filters and differential Kalman Filters.[7]

To briefly describe the methodology, let us consider a dynamical system $\dot{x} = f(t, x)$ and the associated flow map $\varphi(t; t_0, x_0) = x_t$ which give us the position at time t of a particle that at time t_0 is at x_0. As it has been stated, our objective is to propagate a full neighborhood U of x_0, i.e. to compute $\varphi(t; t_0, U)$. For this purpose, the initial condition x_0 is replaced by a simple polynomial that parameterizes its neighbourhood: $P_{t_0,x_0}(\xi) = x_0 + \xi = x_0 + (\xi_1, \ldots, \xi_n)^T$.

Then we can select any ordinary differential equation integrator (RK, Taylor, symplectic,...) and to use it to propagate the polynomial. We note that, since the initial condition is a polynomial, all the computations required in the propagation method have to be done using polynomial algebra, i.e. the algebraic operations are done using truncated polynomials up to a certain order.
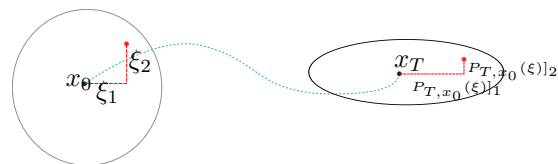

Figure 1: Schematic idea of the Jet Transport.

In this way we obtain the expression of the neighbourhood U propagated at time t by means of truncated Taylor's series up to order n, $P_{t,x_0}(\xi)$. These series give us the state of the particle, that initially is at $x_0 + \xi$, at time t, i.e. $P_{t,x_0}(\xi) = \varphi(t; t_0, x_0 + \xi)$.

Using this procedure the time required for Monte Carlo simulations can be dramatically reduced since now the propagation of an orbit is just a mater of evaluating a polynomial (of course, as a minor drawback, the time to compute the propagation of the neighbourhood is longer than the required for a single trajectory). Moreover, this

[*]Universitat de Barcelona, Spain, daniel@maia.ub.es

[‡]IEEC & Universitat Politècnica de Catalunya, Spain. josep@barquins.upc.edu

[§]IEEC & Universitat de Barcelona, Spain, gerard@maia.ub.es

procedure also allows the study of the covariance matrix up to high order, due to the fact that the different orders of the final polynomials provide the variational equations up to that order.

As an interesting application of this jet transport methodology, in Alessi et al[1] the authors studied the close approach of the Near Earth Asteroid (NEO) Apophis. More concretely they study the close approach of 2019. Other Apophis encounters have been studied in.[2]

2 Jet Transport

The objective of Jet Transport techniques for the numerical integration of Ordinary Differential Equations (ODEs) is to obtain the solutions of the high order variational equations associated to a certain ODE.

The direct computation of high order variational equations requires a large amount of work just to obtain the system of differential equations that must be integrated. To overcome this difficulty, the basic idea is to propagate, instead of just one initial condition x_0, a full neighbourhood of it, given by a polynomial $P_{t_0, x_0}(\xi) = x_0 + \xi$, where $\xi = (\xi_1, ..., \xi_n)$ represents the deviation with respect to x_0. Then, the ODEs can be integrated using any of the usual methods but instead of evaluating the vector-field that defines the differential equation at a certain state using real arithmetic, polynomial arithmetic must be used to do the integrations.

The procedure requires two main ingredients:

1. *A polynomial algebra package.* The polynomial algebra package has to contain all the basic functions needed for the implementation of the integration method. The usual functions that appear in the package are: addition, product, division, composition of polynomials as well as the elementary functions (trigonometric, exponential, logarithm, ...).

2. *An integration method.* Any standard integration method can be used, for instance a Runge-Kutta, a Taylor method or a symplectic integrator (i.e. leap-frog integrator). The arithmetic of the selected method has to be adapted to the Jet Transport, transforming the standard floating point arithmetics of the numerical integrator by a polynomial arithmetic.

In this section we will show the basic characteristics of the Jet Transport methods. First we will describe the basic characteristics of the polynomial algebra; later we will see how we should mix the polynomial algebra with a Taylor integration method, which is the integrator that has been selected for the computations that follow. Then we will discuss the error estimation and the selection of the step control. Finally other applications of this procedure will be commented.

The polynomial algebra

As already stated, one of the basic ingredients of the Jet Transport is the polynomial algebra. In this section we will explain some procedures and considerations for its implementation. The relevance of the polynomial algebra is due to the fact that any algebraic operation in the method will use it. Some of these questions have been studied by Jorba.[5]

The first question that any polynomial algebra must deal with is how the polynomials are stored and accessed. There are several storage procedures in the literature, each one with its own strengths and weaknesses. Some of them have been developed to deal with sparse polynomials, others are memory efficient and others are fast accessing to the data.

In general, the polynomials that appear when the Jet Transport procedure is applied to the usual vector-fields of Astrodynamics and Celestial Mechanics are not sparse, therefore methods thought for these kind of polynomials are not the best option. Two other storage systems are:

- Nested arrays: this system consist in a nest with a number of arrays as the number of variables of the system. It is a fast system to write, since the coefficients are easily stored using the exponents of the variables. As main drawback, their structure is difficult to insert in a general implementation. The dimension of the dynamical system determines the number of arrays that must be nested and, therefore, they cannot be introduced in a general code.

- Reverse lexicographical order: in a first step the monomials are ordered according to their degree. Inside each degree the following rule is applied: the monomial p_j precedes the monomial p_k if the exponent of the first variable of p_j is higher than the exponent of the first variable of p_k. In case that both monomials have the same exponent for the first (second, ...) variable then the second (third, ...) variables should be used for the comparison. In other words, using the multi-indices $j = \{j_1, \ldots, j_n\}$ and $k = \{k_1, \ldots, k_n\}$ then we say that $j < k$ if the minimum i such that $j_i \neq k_i$ verifies $j_i < k_i$.

The selection of one of these two systems is done depending on the characteristics of the problem. Usually, if the number of variables is small the first method is used; when the number of variables is large, then the second method is preferred since, among other things, makes the code more readable.

Another important question that must be considered is how the polynomial algebra package does the computations associated to the basic operations and functions already mentioned. It is possible to give recursive formulas for all of them, whose output will be a polynomial of a certain degree. In all the cases, the basic idea is always to deduce, order by order, the coefficients of the resulting polynomial. In many cases is useful to take derivatives to easily isolate the coefficients of the different degrees.

Proceeding in this way one can obtain recursive formulas for the addition, the product, the division and some elementary functions (trigonometric, logarithm, exponential, ...). It is also possible to compute the polynomial approximation (up to a certain degree) of the composition of two polynomials as well as the inverse.

The efficiency and accuracy of the resulting polynomial algebra package can be tested against any another package. For our implementation we have used PARI/GP,[6] which is a well tested package with an arbitrary floating point precision. The results obtained with both packages are compared to get the error assuming that PARI results are exact, since they are computed with a higher floating point precision. The comparatives have been done using 1000 different input data series. Table 1 shows the logarithm of the average of the errors (computed as the difference of the coefficients associated to the first two exponents) for some of the basic functions. Observe that the precision of the float point using double representation is of 16 digits. Therefore we cannot expect anything higher to that value.

Adapting a Taylor method

The second ingredient of the Jet Transport is an integration method. Here a wide range of options is available (Runge-Kutta of any order or combination of orders, symplectic methods,...). For this work we used the Taylor integration method implemented by Jorba and Zou[4] (do not confuse with the Taylor expansion of the solutions). In this section we will comment the modifications that have been done in the Taylor method in order perform the Jet Transport.

In principle, once the Taylor integration method is available, the implementation of the Jet Transport can be done just changing all the usual floating point arithmetic by the polynomial arithmetic developed in the previous section. Nevertheless, there is a key point, which is the selection of the integration step-size. This is equivalent to the selection of the step control, i.e. how to estimate the integration error of the procedure.

For a standard Taylor method, at each step the solution can be developed in powers of the step-size h as

$$\varphi(t_n + h; x_n, t_n) = \sum_{i=0}^{n} x^{(i)}(x_n, t_n)h^i,$$

and then an optimal step given by

$$h_{opt} = \min \left\{ \left(\frac{\varepsilon e^2 \|x^{(1)}\|_\infty}{\|x^{(N-1)}\|_\infty} \right)^{\frac{1}{N-2}}, \left(\frac{\varepsilon \|x^{(1)}\|_\infty}{\|x^{(N)}\|_\infty} \right)^{\frac{1}{N-1}} \right\}.$$

can be used.

Note that using this step control we are controlling the amount of information that the two last terms of the polynomials are giving to the final result. The contribution of these last two terms has to be smaller than a certain amount ε. In addition we consider relative errors, instead of absolute errors, since in some situations the values of the variables can be large. It can happen that looking to the absolute errors the corrections done are below the mantissa's precision.

For the Jet Transport, each $x_m^{(i)}$ is a polynomial $x_m^{(i)} = \sum_k c_{m,k}^{(i)} \xi^k$ (where m stands for the index of the variable). Therefore, the control should be done for every coefficient of the polynomial. Using

$$\psi_{m,k}^i = \max_{1 \leq m \leq n} |c_{m,k}^{(i)}|,$$

the optimal step becomes

$$h_{opt} = \min_k \left\{ \left(\frac{\varepsilon e^2 \psi_{m,k}^1}{\psi_{m,k}^{N-1}} \right)^{\frac{1}{N-2}}, \left(\frac{\varepsilon \psi_{m,k}^1}{\psi_{m,k}^N} \right)^{\frac{1}{N-1}} \right\}.$$

In this way, we are controlling all the orders of the Jet. It is known that the value of the high-order terms increases fast. Therefore, if we use an absolute error to control the step-size, the integrator will require a small time-step, slowing down the process without adding new information, because it will be under the mantissa's precision. This does not happen when using the relative error, since then we are looking on the mantissa's precision.

Finally, let us add some comments about the sizes of the boxes that can be propagated. In the same way that for the step control, there is a domain where the propagation obtained by the Jet Transport has truncation errors and not errors produced by the method. The problem consist in how can we estimate this domain. In analogy with the step-control selection, some estimations on the box-size can be done using the higher order terms on the final jet. Assuming that at the end of the integration the jet can be written as

$$\varphi(t; x_0 + \xi, t_0) = P_{t_0, x_0}^t(\xi) = \sum_{|k| \leq n} a_k \xi^k,$$

3

Order	power	division	sinus	cosinus	exponential	logarithm
0	-14.42	-15.85	-16.78	-16.50	-17.57	-14.96
1	-15.02	-15.51	-15.80	-15.87	-18.16	-14.99
2	-14.73	-15.07	-15.07	-15.10	-16.77	-14.78
3	-14.52	-14.51	-14.46	-14.45	-15.56	-14.31

Table 1: This table gives, for some basic operations, the logarithm of the mean differences of the coefficients associated to the first two exponents, computed using the developed polynomial algebra and PARI.

then, a straightforward option is to select the size of the box in such way that the last term of the jet does not add more than a certain tolerance to the total addition ε_{jet}, i.e:

$$a_k \xi^k \leq \varepsilon_{\text{jet}}.$$

Assuming that the box has to be of the same size for every direction we get that

$$\xi_{\text{max}} = \min_{|k|=n} \left(\frac{\varepsilon_{\text{jet}}}{a_k} \right)^{1/k}.$$

Applications

The Jet Transport can be applied in different fields and situations. For instance, doing a composition with a time correction function, it is possible to obtain a Poincaré map representation of a flow by just evaluating the polynomial. Once the Poincaré map has been obtained, then is easy to find periodic points as well as to study their stability. In case that the resulting point is hyperbolic, it is possible to determine approximations of its invariant stable and unstable manifolds. In a similar way, the Jet Transport can also be used to compute normal forms.

3 Application Examples

In this section we show the Jet Transport applied in two different scenarios. In the first one we consider a problem of hazard collision between two satellites and try to measure this risk. In the second one we look for invariant manifolds structures of a periodic orbit of the RTBP.

3.1 Measuring satellite risk collision

The jet transport is very suitable to measure collision risk between satellites or between catalogued space debris and a satellite.

Uncertainty regions are represented as boxes from the jet transport point of view. Once the initial uncertainty box is propagated, we can determine the probability distribution of the final states of the satellites as a function of the initial distribution. In particular, if we do the jet propagation for two different satellites, we can run a fast Monte Carlo simulation to compute statistics about the proximity distance.

Let us consider a case example consisting of two satellites in circular orbits that are going to collide after a given time T_c. Assume that their initial states are given by X_1 and X_2 and, in addition, let us consider that both orbits have a similar period so they are going to have some other close approaches before collision. Let us call T_i the corresponding time of these close approaches (we include the value of i such that $T_c = T_i$).

The procedure we are going to follow to study this case is:

1. Using the jet transport, we propagate the neighborhoods of both satellites to a time T_i. This means to compute the polynomial $P_1(\xi)$ (resp. $P_2(\eta)$) that gives us the state of the first (resp. second) satellite at time T_i when $\xi = 0$. Other values of ξ (resp. η) of the jet provide us the state of the corresponding satellite at time T_i for initial conditions $X_1 + \xi$ (resp. $X_2 + \eta$).

2. We take random initial conditions for the variables ξ and η following the probability distribution assumed in the initial uncertainty region (for instance a uniform or a Gaussian distribution).

3. We compute the distance of the two propagated satellites trajectories at time T_i. This means to compute the distance in the configuration space: $\|P_1(\xi) - P_2(\eta)\|_2$.

4. We repeat steps 2 and 3 to obtain a representative sampling for statistics (note that since the propagation is obtained as the result of an evaluation of a polynomial each sample computation is very fast).

As a further remark we note that in step 3, when computing the distance between satellites corresponding to selected values of ξ and η in the initial uncertainty regions, the propagation time plays a role. Near T_i we can find a value of time where the propagated states are closer than

4

they are at time T_i, where the jet has been computed. This is, for each pair of initial conditions we have a time value, near T_i, where the minimum distance is attained. To address this issue we introduce a time coordinate in the final box, also in a polynomial way, and we find the particular time value where the minimum distance is attained using a simple Newton method.

With the sampling results obtained we can compute some statistic indicators like its first moments (mean, standard deviation, skewness and kurtosis). These are reflected in the table of Figure 2 corresponding to different close approaches. Additionally, the same figure also shows frequency histograms of the minimum distance together with the normal distribution obtained using the mean and the standard deviation from the sampling.

As we can see in the figure, three of four approaches have a mean distance of more than 40 kilometers while for the remaining one, corresponding to the third close encounter, the mean distance is about 500 meters. This third approach is the one corresponding to the real impact and we note that its mean is not zero since the minimum distance for each sample cannot be negative. Analyzing the second indicator, the standard deviation, the longer the integration time the larger the standard deviation we find. This fact has also intuitive sense since for longer time integrations the uncertainty region increases and therefore there are more values in the uncertainty zone far away from the center of the propagation.

The skewness, or third moment, seems to be the more relevant statistic indicator. In the colliding case it is high, while in the other ones it is close to zero. Intuitively this indicator is associated to the symmetry of the distribution. Positive values indicate that the samples are displaced to the left with respect to the normal distribution while negative ones indicate that they are displaced to the right. A zero value indicates that the samples follow a symmetric distribution. In our case example, to the non colliding encounters correspond very small skewness values, pointing to symmetric distributions. However, in the colliding scenario we have a large skewness indicating that there are more samples in the left part of the distribution. This lack of symmetry indication is reinforced by the fact that in a close encounter the mean distance of the distribution is small and we cannot have samples with negative distances in the histogram.

As for the last indicator considered, the kurtosis or fourth moment, we have to say that usually it doesn't give any further information and similar values are found for all the scenarios.

Then, to summarize the results of Figure 2 in a rough way, we mainly see that the normal distribution agrees quite well with the histogram for the non-colliding sce-

narios. On the other hand, for the colliding case it appears unbalanced to the left and this fact agrees with the skewness results.

3.2 Invariant structures in the CRTBP

Although the objective of this section is to determine invariant structures in non-autonomous differential systems, extensions to autonomous systems can also be done. First, we will start studying the simple pendulum to show some different procedures that can be used for the computation of the invariant structures, later we will move to the circular restricted three-body problem (CRTBP), Earth-Moon case, to show how we can determine invariant manifolds which play an important role in the study orbits between the two primaries.

For the above purpose, we want to apply the Jet Transport technique to the ideas of G. Haller for the determination of the Coherent Lagrangian Structures (LCS) introduced in.[3] In a naive way, the LCS are manifolds that maximize the relation between the expansion rates along the normal and tangent spaces. This relation is determined by means of the eigenvalues and eigenvectors of the Cauchy-Green tensor ($C = M^T \cdot M$, where M is the State Transition Matrix). With the above information one can determine surfaces for which the normal expansion along the orbits of the surface is bigger than the tangent to the orbit expansion.

As first example, consider the simple pendulum, whose adimensional equations of motion are

$$\ddot{x} = -\sin x.$$

Given an initial condition x_0 in the phase space, define $\vec{t}_0$ as the tangent vector to the orbit and $\vec{n}_0$ as the normal vector to the tangent one at x_0. Analogously, define $\vec{t}_T$ and $\vec{n}_T$ as the tangent and normal vectors at x_T at time T. The idea is to propagate a normal vector to the orbit to the normal space defined at x_T. For this purpose, we can use the same kind of Jet Transport expansion in both position and time ($P_{t,x_0}(\xi, \tau)$). Once we have this expansion, we propagate the polynomial in the variables ξ such that $\xi = s_0 \vec{n}_0$, obtaining as many polynomials in τ as variables has the differential system. Finally solve the system of equations

$$x_T + \sum (s_T)_i (\vec{n}_T)_i = P_{T,x_0}((s_0)_i (\vec{n}_0)_i, \tau),$$

in order to arrive to the new normal space. This system can be solved using Newton's method. Observe that, in general, it is solvable since we have as many unknowns ($\tau, (s_T)_i \ \ i = 1, ..., n-1$) as equations.

Approach	mean	standard deviation	skewness	kurtosis
First	49041.814935	92.760486	0.010182	-0.119546
Second	47710.973011	141.445321	0.034857	-0.133981
Third	545.739802	359.16694	0.634560	-0.128865
Fourth	44475.298463	376.657252	0.045448	-0.120202
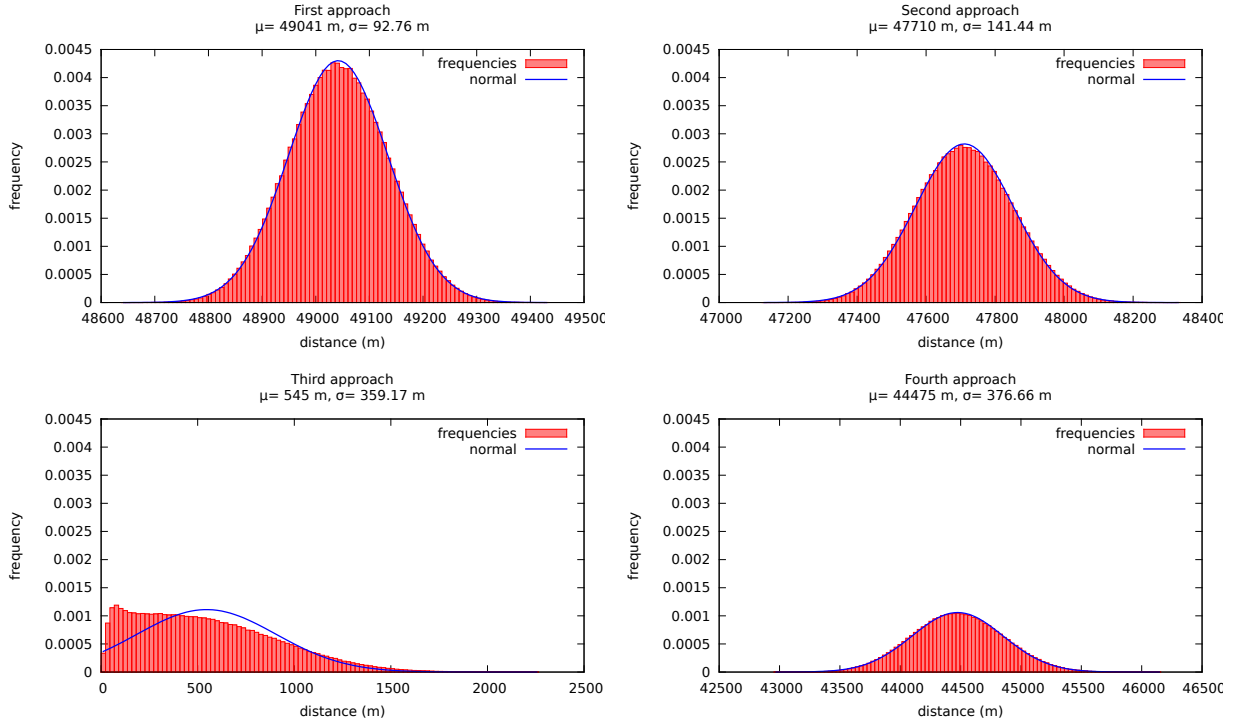
Figure 2: **Top:** The table shows some statistic indicators for the case example corresponding to collision risk of two satellites and four close approaches. **Bottom:** Frequency histograms of distances for the samples. From left to right and top to bottom, the first, second, third and fourth encounters are represented. As a reference, the blue line shows a normal distribution with the same mean and standard deviation as the corresponding samples.

Once the propagation to the normal space is found there are different parameters that can be considered for our goal:

- Distance in the normal space ($s_1(s_0)$). Is the Euclidean distance between the propagated point in the normal space and the center of the box. If this distance is bigger than the initial one then the normal direction is expansive, otherwise is contractive.

- Time of arrival ($\tau(s_0)$). Is the time needed to arrive from $P_{T,x_0}(x_0 + (s_0)_i \cdot (n_0)_i)$ to the normal space. In this kind of plots we are looking how far is the propagation of the normal to the new normal in terms of time. In some way we are looking to the tangential direction.

- Tangential distance ($\bar{t}(s_0)$). Is the distance from $P_{T,x_0}(x_0 + (s_0)_i \cdot (n_0)_i)$. Somehow it is related

to the time of arrival $\tau(s_0)$.

- Tangential projection ($\bar{s}_1(s_0)$). Is the distance from the projection of $P_{T,x_0}(x_0 + (s_0)_i \cdot (n_0)_i)$ into the normal space to the propagated center of the box x_T.

Figure 3 shows the values of $s_1(s_0)$ and $\tau(s_0)$ in the pendulum taking as the initial center of the box the point $(x_0, \dot{x}_0) = (0, 1.5)$ and evaluating the boxes after half a revolution. We can observe how when the initial normal space is close to the separatrix both quantities explode. This fact is explained because during half a revolution of the central point, the points close to the separatrix are still far from the normal space and they will need some extra time to arrive. Therefore, this method is giving some approximation to know where the separatrix (and hence the manifold) is.
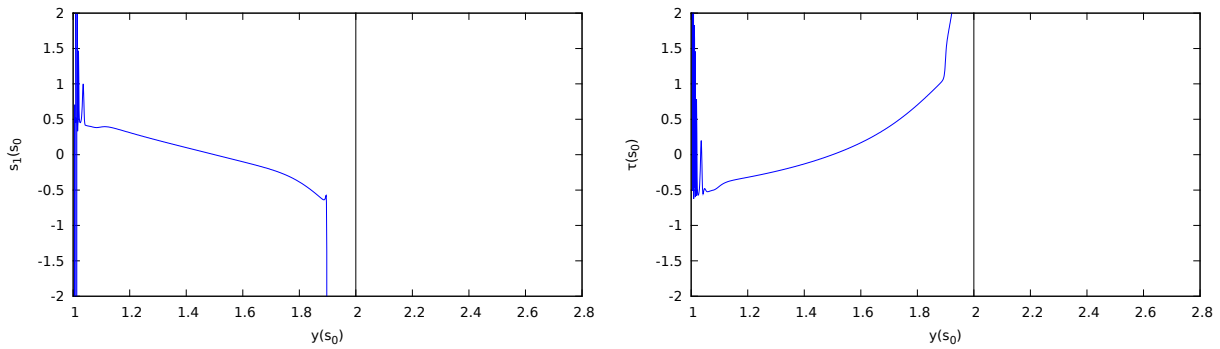
6

Figure 3: **Left**: Representation of the function $s_1(s_0)$ for the initial point $(0, 1.5)$. The x axis is parameterized by the position that corresponds to $x_f + s_0 \vec{n}_f$ in the vertical component. In that way, the separatrix is located at $y(x_0) = 2$ (vertical line). The integration is done for half a revolution of the center of the box. **Right**: Function $\tau(s_0)$ for the same initial points, parameterization and final times.

The next example has more degrees of freedom. The planar CRTBP which is a four dimensional problem, therefore the normal spaces are 3-dimensional and we will not be able to visualize properly the previous indicators.

In order to reduce the number of degrees of freedom, the following can be done:

- Fix an energy level. In this way, the dimensions of the normal spaces at the initial and final points is reduced in one unit.

- Measure the distance from the center of the box, at the point x_T, to the propagated point in the normal space. In that way we reduce from a 2-dimensional normal space to a 1-dimensional space. Here several distances can be used: the Euclidean distance $d_1 = \|(x, y, \dot{x}, \dot{y}\|_2$, the distance in the configuration space $d_2 = (x^2 + y^2)^{1/2}$, or a mixed distance in the configurations and velocity spaces $d_3 = ((x^2 + y^2)^{1/2} + (\dot{x}^2 + \dot{y}^2)^{1/2}$.

With this two reductions we can parameterize the initial normal space using two variables and look at the distance in the final normal space, which can be easily visualized.

For a fixed initial state x_0 and assuming that the propagation using the Jet Transport, $P_{T,x_0}(\xi)$ has been done, an algorithm to detect invariant structures is the following:

1. Compute the normal spaces to the orbit at x_0 and x_T ($\mathcal{N}_0$ and $\mathcal{N}_T$, respectively) using a Gram-Schmidt procedure. Each normal space will be determined by three vectors $n_i \ i = 1, 2, 3$. Then, any point $x \in \mathcal{N}_0$ can be written as

$$x = x_0 + \alpha n_1 + \beta n_2 + \gamma n_3.$$

2. Select those points in the normal space which are in the same energy level of x_0. To do this, one must:

   - Fix $\alpha = \alpha_i$ and $\beta = \beta_j$.
   - Solve the equation $E(x(\alpha_i, \beta_j, \gamma)) - E(x_0) = 0$ and obtain $\gamma = \gamma_{ij}$ using Newton's method.

3. Propagate the point $x(\alpha_i, \beta_j, \gamma_{ij})$ (i.e. evaluate the polynomial $P_{T,x_0}(\xi)$ with $\xi = \alpha_i n_1 + \beta_j n_2 + \gamma_{ij} n_3$) . Again using Newton's method, determine the intersection of the orbit with $\mathcal{N}_T$.

4. Compute the relation between the final distance to x_T and the initial one to x_0. We will denote this distance $r(\alpha, \beta)$.

Then plots of the triplets $(\alpha_i, \beta_j, r(\alpha_i, \beta_j)$ reproduce the plots obtained for the pendulum. Alternatively, the coordinates x, y can be used instead of α, β, since they give more intuition in the problem. Observe that, in almost all the cases, for every pair α, β we have a unique x, y pair.

Figure 4 shows plots of the triplets $(x(\alpha, \beta), y(\alpha, \beta), r(\alpha, \beta))$ for forward and backward integrations. Superimposed it also shows the intersection of the invariant manifolds with the initial normal space $\mathcal{N}_0$. The central point for the boxes corresponds to a Lyapunov periodic orbit around L_1. Unlike in the previous case, now the manifolds appear as the minima of the ratio of distances. This fact is due to the existence of stable and unstable manifolds in the same neighbourhood. Those points which are close to the stable manifold will be close to the periodic orbit during a long time span and, even more, they will get closer. Points not close to the stable manifold will quickly depart from the periodic orbit due to the effect of the unstable orbit. For backwards integrations the manifolds exchange their roles, the unstable manifold will be detected since points around it will be the ones attracted to the periodic orbit points not close will go way.
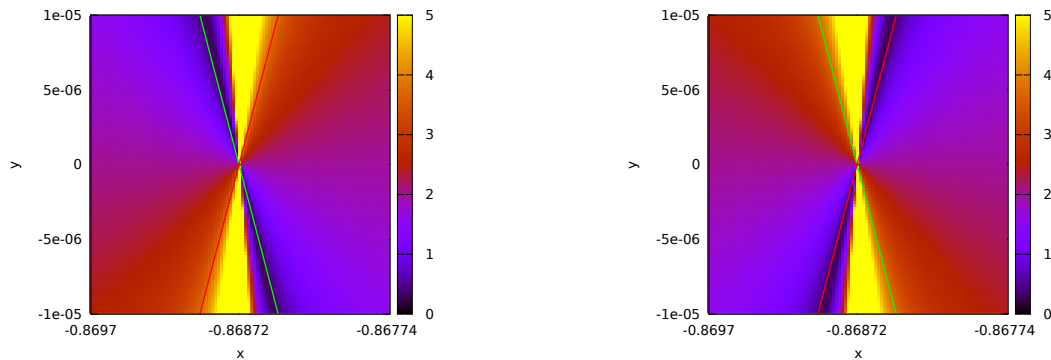
7

Figure 4: Relation between the final and the initial distances (using the $d_2 = (x^2 + y^2)^{1/2}$ distance) with respect the coordinates x, y using forward integration (left) and backward integration (right). The initial central point is a point in a Lyapunov periodic orbit around L_1 with energy $E = -1.583043$. The final time of integration is $T = \frac{-1}{10}t_p \approx -0.283228$ and $T = \frac{1}{10}t_p \approx 0.283228$. Superimposed the x, y coordinates of the intersection of the invariant manifolds with the normal space $\mathcal{N}_0$, red the unstable manifold, green the stable one.

Proceeding in this way, we are able to detect invariant manifolds in a neighbourhood of the periodic orbit. If we are far away, the propagation using the Jet Transport is not good enough to accurately compute the manifolds.

4   Conclusions

In this paper we present the jet transport propagation and some applications. Opposite to the traditional propagation schemes that propagate single states, this tool allows us to integrate full neighborhoods of points and in this work it has been applied in two completely different scenarios. The first one corresponds to the study of collision risk between a couple of satellites using a speeded up Monte Carlo simulation. The preliminary results that we present show that the main statistical indicators are the mean distance and the skewness. Small mean distances and big skewness values point to the existence of a collision risk, while the other indicators studied are not conclusive at all with respect to this point.

The second application points towards the detection of Lagrange coherent structures in dynamical systems. We have seen that using the jet transport it is possible to detect the invariant manifolds of a periodic orbit of the RTBP, at least locally. In this case the jet transport is used in order to analyze how the normal space to the orbit expands or contracts.

Acknowledgements

References

[1] E.M. Alessi, A. Farrès, A. Vieiro, À. Jorba, C. Simó *Jet transport and applications to neo's* Conference proceeding

[2] F. Bernelli-Zazzera, M. Lavagna, R. Armellin, P. Di Lizia, F. Topputo, M. Berz, K. Makino and R. Jagasia *NEO Encounter 2029 Orbital Prediction via Differential Algebra and Taylor Models* ESA Final Report, Ariadna ID: AO/1-5680/08/NL/CB

[3] G. Haller, G. Yuan *Lagrangian coherent structures and mixing in two-dimensional turbulence* Phys. D 147:352-370, 2000

[4] À. Jorba, and M. Zou *A software package for the numerical integration of ODE's by means of high-order Taylor methods* Exp. Math., 14(1):99-117, 2005

[5] À. Jorba *A methodology for the numerical computation of normal forms, centre manifolds and first integrals of Hamiltonian systems* Exp. Math. 8(2):155-195, 1999i

[6] PARI/GP, version 2.5.3, Bordeaux, 2012, http://pari.math.u-bordeaux.fr/.

[7] M. Valli, R. Armellin, P. Di Lizia, M. Lavagna *A Gaussian Particle Filter based on Differential Algebra for Spacecraft Navigation* IAC-12-C1.1.1